Design of Biodegradable Mg Alloy for Abdominal Aortic Aneurysm Repair (AAAR) Using ANFIS Regression Model

RANIA E. HAMMAM[1], **AHMED A. A. SOLYMAN**[2], **MOHAMMED H. ALSHARIF**[3], **PEERAPONG UTHANSAKUL**[4], **(Member, IEEE), AND MOHANAD A. DEIF**[1]

[1]Department of Bioelectronics, Modern University for Technology & Information (MTI), Cairo 11585, Egypt
[2]Department of Electrical and Electronics Engineering, Istanbul Gelisim University, Istanbul, 34310 Avcilar, Turkey
[3]Department of Electrical Engineering, College of Electronics and Information Engineering, Sejong University, Gwangjin-gu, Seoul 05006, South Korea
[4]School of Telecommunication Engineering, Suranaree University of Technology, Nakhon Ratchasima 30000, Thailand

Corresponding authors: Mohammed H. Alsharif (malsharif@sejong.ac.kr) and Peerapong Uthansakul (uthansakul@sut.ac.th)

ABSTRACT Abdominal aortic aneurysm (AAA) is among the most widespread and dangerous diseases that may cause death. Recently, Endovascular Aneurysm Repair outperformed open aortic surgery, since it is a safe and reliable technique where a stent graft system is placed within the aortic aneurysm. It was aimed to design an Mg biodegradable alloy with bio-friendly alloying elements that enhance the corrosion resistance and mechanical properties of the alloy for the design of stents for Abdominal Aortic Aneurysm (AAA) repair. Adaptive Neuro-Fuzzy Inference System (ANFIS) was proposed for the design of the Mg alloy and compared to other traditional machine learning regression models (Multiple Linear Regression (MLR) and Gradient Boosting (GB). The dataset utilized in this work consisted of 600 samples of Mg alloys that were collected from the mat web database and additional papers from Google Scholar. The results revealed the superior prediction capability of the ANFIS model since it attained maximum R^2 scores of 0.926, 0.958, and 0.988 for the prediction of UTS, YS, and Ductility respectively. Furthermore, the ANFIS model was capable of designing an Mg biodegradable alloy having a UTS, YS, and Ductility of 346.148 Mpa, 230.8 Mpa, and 15.4% respectively which are excellent mechanical properties satisfying vascular stents requirements The ANFIS model can be further applied to speed up the design of other alloys in the future for various medical applications, reducing the time, cost, and effort of large searching space.

INDEX TERMS Abdominal aortic aneurysm, ANFIS, biodegradable, gradient boosting, Mg alloy.

I. INTRODUCTION

An aortic aneurysm is an enlargement of the aorta, causing the diameter to increase by at least 50% of its normal size [1]. They usually occur in the abdominal aorta and thoracic aorta, as well as in the arteries located at the base of the brain and legs [2]. Aortic aneurysms can weaken the wall of the aorta and increase the risk of aortic rupture. When a rupture occurs, excessive internal bleeding will occur, and if it is not treated directly, shock and death may occur.

Abdominal aortic aneurysm (AAA), which is the most common and fatal diseases, has been treated in the early

1950s by replacement of the diseased part of the aorta by a synthetic graft through open surgery [3], [4]. However, the mortality associated with this process has been reported to have reached 8%, and 10% of patients may experience cardiac complications, respiratory and renal failure [5], [6]. In the early 1990s, the placement of a graft within an AAA was a suitable alternative to open surgery and proved to be a safe and reliable technique [7].

In 2003, endovascular aneurysm repair (EVAR) was superior to open aortic surgery in repairing abdominal aortic aneurysm (AAA) [8]–[10]. In 2010, EVAR accounted for 78% of all endovascular AAA repairs in the United States [11]. Currently, EVAR is the most widely used method for the treatment of aortic aneurysm disease. Endovascular

The associate editor coordinating the review of this manuscript and approving it for publication was Taous Meriem Laleg-Kirati.

aneurysm repair (EVAR) is a process in which a stent graft system is placed in an aortic aneurysm with the help of a thin, flexible plastic tube called a delivery catheter to protect the diseased or damaged area from blood circulation. Therefore, the purpose of this procedure is to strengthen the aortic wall and help protect the aneurysm sac from blood pressure, thereby preventing the aortic wall from rupturing. The advantage of this method is that there is no need to remove any tissue from the aorta and the stent recovery time is faster because it is less invasive than open surgery.

A stent-graft is an intraluminal device composed of a metal supporting framework (typically Stainless Steel or Nitinol) and a synthetic graft material (commonly expanded Polytetrafluoroethylene (PTFE) or Polyester) (PET, Dacron). The stent can be placed inside, outside, or inside the graft material, and it can run the length of the graft or just the ends. The stent serves as an arterial attachment mechanism, providing structural support for both the graft and the treated vascular segment. The graft creates a new channel for blood flow, protecting the damaged artery from pulsatile blood pressure [2] [12]. A. Polanczyk, *et al.* [13] performed a study to investigate the influence of a stent-graft on the pulsatile blood hemodynamic changes in the abdominal aortic aneurysm (AAA) of some patients before and after stent-graft placement. The authors concluded that the presence of the stent-graft decreased blood vessel wall deformation and significantly minimized the influence of frequency of pulsation and therefore reduced the risk of aortic rupture.

Several studies have been conducted on biodegradable stents for cardiovascular applications [14]–[16] and Abdominal Aortic Aneurysm (AAA) repair [2], [17], [18]. Stainless Steel and Nitinol stents [19], [20] were commonly used due to their mechanical properties, biocompatibility, and good corrosion resistance. However, once inside the patient's body, metal ions may be discharged due to corrosion and/or wear, causing an inflammatory response in the surrounding tissues, causing invasive subsequent procedures to remove. To minimize the pain and medical costs for patients, biodegradable metal stents are introduced to replace the traditional non-degradable metal stents.

Many researchers in the biomedical and materials science disciplines are interested in biodegradable stents because they can perform their job for the predicted amount of time and then degrade naturally. The biodegradable stent in the stent-graft system acts as mechanical support or scaffold for fixation of both the graft and the aorta vessel wall. It then degrades over time gradually while being metabolized in the body and replaced by the healed host aorta tissue, thus reducing the long-term harms caused by permanent non-degradable stents. Finally, the graft should reach a stage where it integrates with the host aorta and is biologically fixed on the vascular wall helping to prevent the aortic rupture.

Recently Magnesium biodegradable alloys have been proposed as a promising class of biodegradable metallic stents [21]–[23] due to their excellent biocompatibility, mechanical performance, and biodegradation [24]–[26]

inside the human body. Mg is also one of the trace elements found in the human body, which helps to maintain the body healthy by performing different intracellular physiological tasks, stimulating bone formation, and improving cell adhesion to biomaterials. Furthermore, corrosion products of Mg alloys are nontoxic and can be absorbed by the body or expelled by the surrounding tissues and metabolic system [27]. The primary drawback of using Mg alloys is their high corrosion rates in the physiological environment, which results in rapid degradation, loss of mechanical integrity early in the degradation process, and implant failure before vascular remodeling [28], [29]. In-vivo investigation on the safety, mechanical performance and degradation of Mg stents were carried out in several works [30] [31]. B. Grüter et al[30] reported that animals treated with Magnesium stents showed better aneurysm healing compared with those without stents. They concluded that Bioabsorbable magnesium stents offered a promising approach for the development of future endovascular devices in aneurysm therapy. Patent US 2010/0256728 A1[31] presented a stent graft system comprised of biodegradable Mg - Zn alloy metal stent and biodegradable polymer (polycaprolactone) graft and was then applied to several patients suffering from early stage aortic aneurysm and a patient that had a slight tear in the aorta. After 6 months implantation of the stent graft system, the aneurysm has totally healed and the stent graft has begun to degrade inside the body. Later after a year, the stent graft was completely degraded inside the body, saving patients from having to deal with any complications and lifelong monitoring related to having a permanent metal device in his/her body.

Coating with di-calcium phosphate dehydrate (DCPD) [32], Polymer deposit coating [33], Alkali-Heat treatment [34], and alloying with other elements such as aluminum, manganese, and rare earth elements [35] have all been used to increase the mechanical strength, improve the corrosion behavior and decrease the rate of degradation of Mg alloys. Aluminum (Al) is a common alloying element that is added to Mg alloys in amounts ranging from 1 to 5% to improve corrosion and mechanical qualities by reducing particle size [36]. Calcium (Ca) concentrations up to 0.5% help to stabilize the grain size whereas percentages above that value sped up the corrosion rates of Mg alloys so it should not exceed 1% [37]. Manganese is another important element in magnesium alloys, and its concentration of less than 0.4% reduces the grain size and improves the tensile strength and fatigue life of Mg-Al-Mn alloys [38]. Also, percentages less than 9% lithium (Li) can improve the ductility, corrosion resistance, and formability of Magnesium alloys [38]. Song *et al.* [39] reported that Mn improves the corrosion resistance of Aluminum-Magnesium alloys. However, a higher concentration of Mn will reduce the corrosion resistance, because a large number of intermetallic phases of Mn-Mg-Al are produced, which can be subjected to galvanic corrosion. The addition of zinc (Zn) also helps to improve the corrosion resistance of Magnesium alloys. Cai *et al.* [40]

mentioned that the addition of Zn as high as 5% by weight to the Mg improves the corrosion resistance and mechanical properties of the alloy. Song and St. John [41] suggested in their work that the addition of Zr of a 0.6 wt % favored the corrosion resistance of the Mg-Zn alloy containing rare earth elements since Zr provides a grain refinement effect due to the formation of continuous layers of corrosion-resistant intermetallic rare earth phases around grain boundaries. Rare-earth elements (REEs) including Y (Yttrium), Nd (Neodymium), Gd (Gadolinium), Ho (Holmium) and La (Lanthanum) are commonly added to Mg alloys as hardeners that provoke the strength and corrosion resistance by both solid solution and precipitation hardening. Liu *et al.* [42] reported that when 0.5% La is added to AZ91 alloy, the corrosion rate decreased, while Zhou *et al.* [43] revealed the effect of adding 0.24% by weight and 0.44% by weight of Ho, which also significantly reduced the corrosion rate of the AZ91D magnesium alloy. Kannan *et al.* [44] reported that the corrosion resistance of EV31A Mg alloy was improved by addition of 2.35% Nd and 1.3% by weight Gd.

To identify the best Mg alloy with good mechanical properties, one must first produce many alloys with various alloying element compositions, which are generally done by trial and error, and then test each of them in a large searching space. This is a time-consuming and expensive treatment. Machine learning is a promising and efficient technology for reducing the time, cost, and effort required to design new alloys. Machine learning approaches have recently been used in materials science to identify new alloys [45], predict physical properties [46], [47], and predict tensile properties [48].

Therefore, the purpose of this work is to design an Mg biodegradable alloy with bio-friendly alloying elements that lead to improved corrosion resistance and mechanical properties of the alloy for the design of Bioabsorbable stents (BVS) for Abdominal Aortic Aneurysm (AAA) repair. The mechanical properties of the stent should be similar to those of 316L stainless steel, which is the standard vascular stent material [15],[23] [49], in order to achieve appropriate scaffolding. Furthermore, it has been stated that the ideal mechanical properties for Biodegradable stents include Yield Strength (YS) larger than 200 MPa, Ultimate Tensile Strength (UTS) greater than 300 MPa, and an Elongation greater than 15-18 percent [50], [51].

This study presented the Adaptive Neuro-Fuzzy Inference System (ANFIS), Multiple Linear Regression (MLR), and Gradient Boosting (GB) Regression models for the design of an Mg biodegradable alloy for AAA repair. Furthermore, an evaluation was conducted on the presented models using the R^2 score to attain the best suitable model having the highest efficiency and capability of designing the Mg alloy. A YS greater than 200 Mpa, UTS greater than 300Mpa, and Ductility (Elongation) higher than 15 % were chosen as mechanical properties appropriate for the design of endovascular stents. The compositions of alloying elements were selected from previous literature according to the optimum concentrations that lead to improved mechanical and corrosion resistance

properties and therefore controlled degradation rates of Mg alloys.

II. METHODOLOGY AND DATASET PREPARATION
A. PRELIMINARIES
1) ADAPTIVE NEURO-FUZZY INFERENCE SYSTEM (ANFIS) REVIEW

The Neuro-Fuzzy Inference System (NFIS) combines the Fuzzy logic system (FLS) and the artificial neural networks (ANN). Combining this method with neural networks produces significant results, which can provide a rapid and accurate prediction of biodegradable Mg alloys having certain mechanical properties for various medical applications. The adaptive network-based fuzzy inference systems (ANFIS) are used to unravel difficulties associated with parameter recognition issues [52]. This parameter recognition is achieved by integrating the back-propagation gradient descent and the least-squares approach via a hybrid learning law.
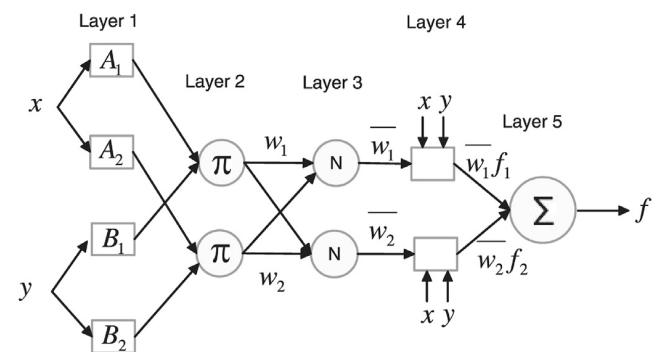

FIGURE 1. Structure of the ANFIS network.

ANFIS is a graphical network representation for a Takagi-Sugeno-type fuzzy inference system with neural learning capabilities. Fig. 1 depicts the architecture of the ANFIS. The circular nodes show fixed nodes, whereas the square nodes represent nodes with parameters that must be learned.

a: ANFIS ARCHITECTURE

ANFIS system architecture comprises five layers, as stated in Figure 1.

Layer 1: Fuzzification layer is the first layer. It comprises input variable MFs (Member-ship functions) and provides inputs to the next layer. Every node *i* in this layer is a square node and is shown in equations (1) and (2):

$$O_{1,i} = \mu_{A_i}(x) \quad for\ i = 1, 2 \tag{1}$$

$$O_{1,i} = \mu_{B_{i-2}}(y) \quad for\ i = 1, 2 \tag{2}$$

where $\mu_{A_i}(x)$ and $\mu_{B_{i-2}}(y)$ fuzzy membership function (MF).

Layer 2: The second layer in the ANFIS network is the rule layer where it computes the weight for each M. The membership functions are the input values in this layer, and each node multiplies the input and outputs the rule's firing power. This layer's output is given in the equation. (3).

$$O_{2,i} = w_i = \mu_{A_i}(x)\,\mu_{B_i}(y) \quad for\ i = 1, 2$$

$$\tag{3}$$

Layer 3: This layer calculates outputs in normalized firing strength. The ratio of the i-th rule's firing strength to the sum of the rule's firing strengths is used to determine the i-th node.

$$O_{3,i} = \bar{w}_i = \frac{w_i}{w_1 + w_2} \tag{4}$$

where $\bar{w}_i$ is referred to as the normalized ?ring strength.

Layer 4: calculates parameters function of layer 3 outputs.The total output is calculated in this layer as the summation of all incoming signals as shown in equation (5).

$$O_{4,i} = \bar{w}_i f_i = \bar{w}_i (p_i x + q_i y + r_i) \tag{5}$$

where $\bar{w}_i$ is the layer 3output, and $(p_i x + q_i y + r_i)$ is the parameter set. The succeeding parameters refer to the parameters in this layer.

Layer 5: In this layer, a single node calculates the entire output as the sum of all input signals, which is stated as

$$O_{5,i} = \sum_i \bar{w}_i f_i = \sum_i \frac{w_i f_i}{w_i} \tag{6}$$

Ten different types of Membership functions (MFs) were investigated to get the best suited ANFIS model [53]. The membership function (MF) is the most important notion in fuzzy set theory; it determines the fuzziness of a fuzzy set. [54], [55]. In order to find the optimal distribution of the MFs, the input-output mapping connection in this work was determined using a hybrid learning algorithm, which is a combination of the backpropagation (BP) algorithm and the least square method (LSM) method [56].

b: HYBRID-LEARNING ALGORITHM
The ANFIS has two classes of tuning criteria, the first layer called the premise, and consequent parameters in the fourth layer[52]. Throughout the learning process, these parameters are attuned until the wanted response of the FIS is accomplished. The ANFIS output can be written as:

$$f = \frac{w_1}{w_1 + w_2} f_1 + \frac{w_2}{w_1 + w_2} f_2 \tag{7}$$

2) MULTIPLE LINEAR REGRESSION
Multiple linear regression (MLR) is a statistical methodology that uses the least square method to describe the linear connection between two or more independent variables and a single dependent variable.

a: REGULARIZATION
Regularization is a strategy for reducing error while also injecting bias into the training set and avoiding overfitting. Ridge regression and LASSO ((Least Absolute Shrinkage and Selection Operator) Regression are two common regularization approaches. LASSO is an effective continuous procedure for estimating and selecting variables [57]–[60].

b: RIDGE
Ridge is a skewed prediction approach that works on the premise of minimizing the sum of residual squares (RSS)

to get the coefficients. The ridge coefficients are calculated using the following equation:

$$\grave{\beta}_{\text{Ridge}} = \arg \underset{\beta}{m} \text{RSS}(\beta)$$

$$= \arg \underset{\beta}{m} \left\{ \begin{array}{l} \sum_{i=1}^{n} \left(y_i - \beta_0 - \sum_{j=1}^{k} x_{ij}\beta_j \right)^2 \\ + \lambda \sum_{j=1}^{k} \beta_j^2 \end{array} \right\} \tag{8}$$

where $\ell_2 = \sum_{j=1}^{k} \beta_j^2$ is the penalty function of the ridge and $\lambda \geq 0$ is the complexity constant that controlling the amount of shrinkage [61], [62]

c: LASSO
The β coefficients can be obtained using this method by solving the following optimization problem:

$$\hat{\beta}_{\text{LASSO}}$$

$$= \underset{\beta}{\text{argmin}} \left\{ \sum_{i=1}^{n} \left(y_i - \beta_0 - \sum_{j=1}^{k} x_{ij}\beta_j \right)^2 + \lambda \sum_{j=1}^{k} |\beta_j| \right\} \tag{9}$$

where $\ell_1 = \sum_{j=1}^{p} |\beta_j|$ is the LASSO penalty function. l_1 penalty is the least-squares fit and shrinks some components of $\hat{\beta}_{\text{LASSO}}$ to zero. The solution to the LASSO method requires quadratic programming [52] [57]

d: ELASTIC NET (EN)
Elastic net is a LASSO variant that is resistant to strong correlations between predictors [55] [63]. The method, which combines the ridge (ℓ_2) and LASSO (ℓ_1) penalties, can be written as follows:

$$\grave{\beta}_{\text{EN}} = \left(1 + \frac{\lambda_2}{n} \right) \left\{ \underset{\beta}{\text{argmin}} \left(\sum_{i=1}^{n} \left(y_i - \beta_0 - \sum_{j=1}^{k} x_{ij}\beta_j \right)^2 \right. \right.$$
$$\left. \left. + \lambda_2 \sum_{j=1}^{k} \beta_j^2 + \lambda_1 \sum_{j=1}^{k} |\beta_j| \right) \right\} \tag{10}$$

3) GRADIENT BOOSTING ALGORITHM
The gradient boosting algorithm designed by Friedman [64] is an ensemble method in which classification and prediction are performed by combining weaker models. This technique has three elements: 1) The loss function that must be optimized. The loss function is an index used to calculate how well the model coefficients fit the data. 2) Weak students, perform classification or prediction (decision tree), 3) Add model, add one tree at a time. The final result is generated based on the average of all weak students. In increasing gradient, weak students work sequentially. Each model tries to improve on the error of the previous model. The n-estimator indicates the number of decision trees employed in the model.
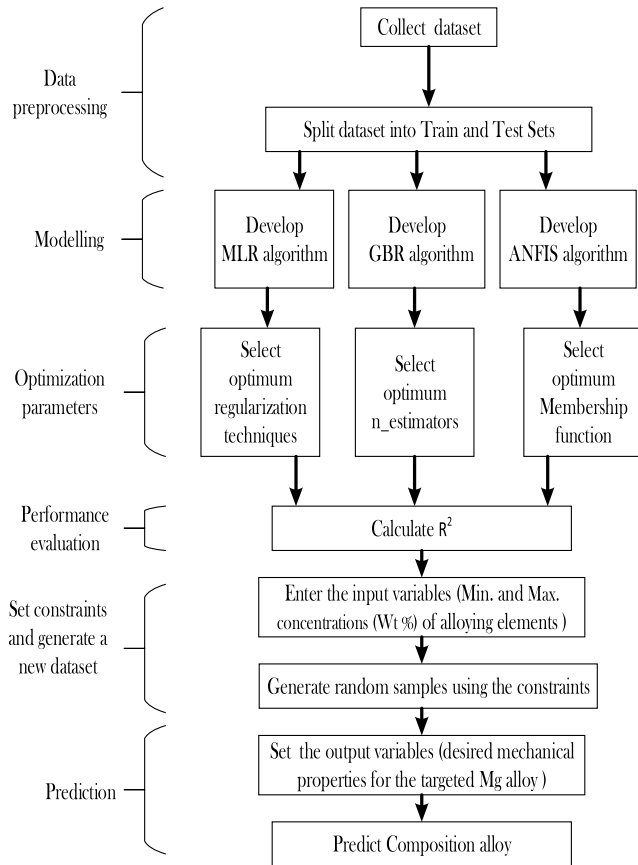
FIGURE 2. Proposed Scheme Methodology.

TABLE 1. Hyper-parameter setting for different classifier algorithms.

Classifier type	Hyper-Parameter	Optional
MLR	Regularization Techniques	LASSO, Ridge, and EN
	Maximum Iteration	1000
XGBoost	Maximum Depth	6
	Learning Rate	0.1
	Number of Estimators	50,100, 200, 300 and 400

B. PROPOSED ALGORITHMS

The proposed method is presented in Fig. 2 which comprised four stages. In the first stage, the dataset containing 600 samples of Mg alloys was collected, preprocessed, and then split into two parts for training and testing the models. The second stage is developing and evaluating the three proposed model algorithms and determining the optimum parameters that produced the best fit models. The third stage is entering the input variables (minimum and maximum compositions (Wt %) of alloying elements composing the targeted Mg alloy) and generating a new dataset. The final stage, which is the most important step is setting the desired output variables (mechanical properties of the targeted Mg alloy crucial for the design of biodegradable stents). The selected best-fit machine learning model is then employed to predict the composition

TABLE 2. Maximum concentrations (weight %) of alloying elements composing the new Mg biodegradable alloy.

Element	Maximum Concentration (Wt %)
Mg	97
Mn	0.4
Al	6
Ca	0.5
Zn	5
Li	9
Zr	0.8
Y	4.5
Nd	4.5
Gd	1.5
Ho	0.44
La	0.5

of the Mg biodegradable alloy having mechanical properties close to the desired output variables out of the newly generated dataset and suitable for vascular stents for AAAR.

1) DATASET SELECTION AND PREPROCESSING

600 samples of Mg alloys were collected from the mat web database and additional papers from Google Scholar. According to previous works, a biodegradable Mg alloy having efficient mechanical and corrosion resistance properties for use in medical applications should contain certain essential elements. Therefore, some columns containing elements like Fe, Ni, Sc, Sr, Er, Tb, Ty were removed from the dataset since they were not from the essential elements in order to increase the efficiency and accuracy of prediction of the proposed models. Consequently, the main elements included in the dataset are Mg (Magnesium), Mn (Manganese), Al (Aluminum), Ca (Calcium), Zn (Zinc), Li (Lithium), Zr (Zirconium), Y (Yttrium), Nd (Neodymium), Gd (Gadolinium), Ho (Holmium) and La (Lanthanum). Duplicate entries were removed from the dataset to get good accuracy for the model. The names of the alloys were removed from the dataset as they were unique and no useful information can be extracted from that column for machine learning. The dataset was then split into two parts, one part was used for training the models while the other part was used for testing the ability of the models to predict the mechanical properties of the Mg sample alloys.

2) MODELLING AND EVALUATION OF THE REGRESSION MODELS

The next step was developing the Adaptive Neuro-Fuzzy Inference System (ANFIS) model and comparing its performance to other traditional machine learning algorithms (Multiple Linear Regression (MLR) and Gradient Boosting (GB) Regression models). The R^2 scores were calculated to evaluate the performance and prediction capability of all presented models. The optimum parameters for all the proposed models were chosen to produce the best fit model, which will be further employed for the design of the targeted Mg alloy. Details of the hyper-parameter settings for the ANFIS model and the other traditional classifier algorithms employed in this work are summarized in Table 1.

The adjusted coefficients of determination $\left(R^2\right)$ were used as cohesion criteria to compare the performance of the models and shown in the following equation:

$$R^2 = 1 - \frac{\sum_{i=1}^{n}(P_i - A_i)^2}{\sum_{i=1}^{n}A_i^2} \qquad (11)$$

P_i and A_i have predicted values, the actual number of the ith record, and n is the total number of records [65]. If R^2 is close to 1, then a high-level correlation is displayed. R^2 shows the percentage variance explained by the model. Models with R^2 higher than 75% are considered excellent.

3) SETTING THE CONSTRAINTS AND GENERATING A NEW DATASET

The third stage of the presented methodology is setting the constraints (input variables) for the models, which comprise the minimum and maximum concentrations (Wt%) of the alloying elements composing the targeted Mg alloy and then generating a new dataset. The minimum concentrations for all alloying elements would have 0 Wt%. The maximum concentrations of the elements were chosen with reference to previous literature. The compositions of the alloying elements that lead to improved mechanical properties of the Mg alloy were shown in the following Table 2. The generated dataset consisted of 1 million samples of Mg alloys.

4) SETTING THE DESIRED MECHANICAL PROPERTIES AND PREDICTION OF THE NEW MG BIODEGRADABLE ALLOY

Finally, the last most essential step is to design a biodegradable Mg alloy having mechanical properties suitable for stents employed in stent graft systems for Abdominal Aortic Aneurysm (AAA) repair. This work focused on three main mechanical properties of Mg alloys, which were Ultimate Tensile Strength (UTS), Yield Strength (YS), and Ductility, also known as elongation. Mechanical properties of YS greater than 200 Mpa, UTS greater than 300Mpa, and ductility (elongation) higher than 15% were set as output variables appropriate for the design of endovascular stents. The most efficient model was selected to predict the composition of the Mg alloy having the desired mechanical properties out of the newly generated dataset. The description of the mechanical properties is explained hereinafter.

a: ULTIMATE TENSILE STRENGTH

is the maximum tensile load that a material can bear until it breaks. It shows the resistance of the material to tensile fracture [66]. It is also the highest point of the stress-strain curve formed after tensile testing. The tensile strength can also be determined using this formula:

$$\sigma_f = \frac{P_f}{A_o} \qquad (12)$$

where P_f is the load at fracture, A_o is the original cross-sectional area, and σ_f is the tensile strength, measured in N/m^2 or Pascals. An ideal Mg-alloy that can be used as an important structuring metal should have UTS higher than the yield strength.

b: YIELD STRENGTH

is the point at which the material begins to deform plastically. Below this point, the material deforms elastically and returns to its original shape after the applied stress is relieved. Yield strength is measured in N/m^2 or Pascals. Materials having high yield stresses are required in orthopedic applications in order to withstand loads without undergoing plastic deformation.

c: DUCTILITY

is the ability of the material to deform plastically without fracture. It can be measured in terms of reduction in area or elongation (% plastic strain at fracture) [67]. An ideal Mg alloy should have a ductility of around 10-15% for it to be considered desirable to create optimum Mg alloys. Ductility or percent elongation can be expressed as

$$\text{Percent Elongation} = \frac{\Delta L}{L_0} \times 100\% \qquad (13)$$

where ΔL is the change in length, L_0 is the original length.

III. RESULTS AND DISCUSSION

The initial goal of this study is to design an Mg biodegradable alloy having improved mechanical properties suitable for the design of biodegradable stents for AAAR. This will be accomplished by developing an Adaptive Neuro-Fuzzy Inference System (ANFIS) model and comparing it with traditional machine learning algorithms (Multiple Linear Regression (MLR) and Gradient Boosting Regression models) to attain the best machine learning technique for the design of the Mg alloy. This will further save time, effort and lead to the precise design of alloys having various medical applications. First, it was important to test the capability and efficiency of the proposed models to predict the UTS, YS, and ductility of the Mg samples in the preprocessed testing dataset by calculating the R^2 scores of the models. The optimum parameters that lead to the best performance in all models were attained by studying the effect of these parameters on the R^2 score of the models. The best fit models were then compared to give an insight into which model performs best for further use in the design of the Mg-targeted alloy.

Fig. 3 shows the effect of membership functions on the R^2 score of the ANFIS model. Three curves were drawn for the three main mechanical properties UTS, YS, and Ductility. It was observed from the curves that the Trainscg membership function (Symbol H) was the best method for ANFIS in predicting the mechanical properties of the alloys with maximum R^2 scores of 0.926, 0.958, and 0.988 for UTS, YS & Ductility respectively. The values of *the*R^2 score for the three mechanical properties for the selected membership functions were tabulated in Table 3. It was also observed that the R^2

TABLE 3. Summary of performance standards for different types of membership functions.

Membership functions (MF)	Symbol	UTS	YS	Duct
Trapezoid-shaped MF	A	0.789	0.820	0.872
Triangular-shaped MF	B	0.804	0.809	0.821
Gaussian MF	C	0.783	0.885	0.777
Gaussian Combination MF	D	0.795	0.810	0.869
Bell-shaped MF	E	0.703	0.793	0.840
Difference sigmoidal MF	F	0.884	0.882	0.616
Product sigmoidal MF	G	0.809	0.711	0.798
Polynomial-Pi MF	H	0.926	0.958	0.988
Z-shape	I	0.736	0.860	0.554
Spline-based curve	J	0.665	0.842	0.496

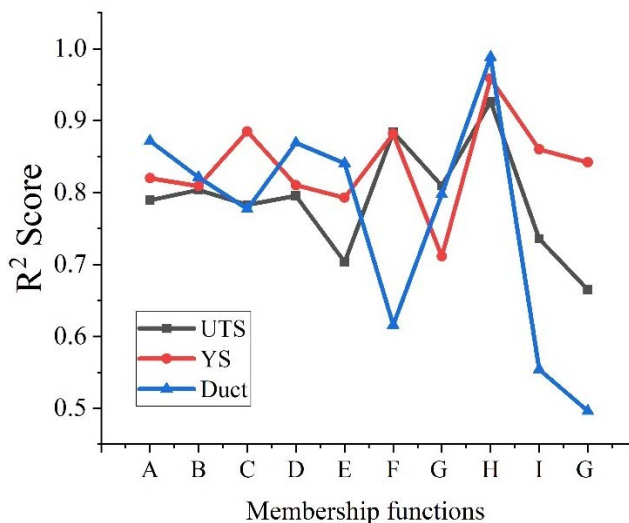**FIGURE 3.** Effect of Membership functions on the ANFIS model Performance.

scores for the Trainscg membership function approached 1 which means the superior performance of the ANFIS model.

Fig. 4 shows the effect of regularization techniques on the R^2 scores of the Multiple Linear Regression (MLR) model. It was clear that the prediction ability of the MLR model for the yield strength (YS) of the Mg alloys using all regularization techniques was the highest, having the maximum R^2 scores. It was also seen that the R^2 scores for the prediction of YS and UTS using the Ridge and LASSO methods were nearly the same, however, there was a clear difference between the two methods in the prediction of ductility since the R^2 score using the Ridge technique was the highest of 0.35. Hence, the Ridge method was chosen to be the best fit regularization technique for Multiple Linear Regression with the more reliable and precise prediction ability.

The influence of the n-estimator parameter on the R^2 scores of the Gradient Boosting regression model was presented in Fig. 5. It was observed that the R^2 scores for the yield strength profoundly increased with the increase in the n-estimator of the model reaching the highest value at an n-estimator of 400. Similarly, the R^2 scores for the ductility also reached the highest value at an n-estimator of 400. However, the ultimate tensile strength attained the highest R^2 score of 0.8 at 100 and it slightly decreased to 0.77 at 400. Accordingly, an n-estimator of 400 was chosen to be the optimum parameter for the Gradient Boosting regression model.

The coefficients of determination R^2 scores for all best-fit models were summed up in Table 4. The results showed that R^2 values for the ANFIS model for the three mechanical properties were above 0.75 and they were very close to 1, which shows the high prediction accuracy of the model. By comparing the ANFIS model with the MLR and GBR regression models, the results confirmed the superior prediction capability of the ANFIS model. The fundamental reason for this is that the ANFIS model combines the benefits of neural network learning capabilities with fuzzy logic principles to construct a grading relationship between input factors and Mg alloy output mechanical qualities. As a result, it was further employed to create the biodegradable Mg alloy with the appropriate mechanical characteristics.

The composition of the generated Mg alloy predicted by the presented ANFIS model was shown in Table 5 and Fig. 6.

It was clear that the generated Mg alloy exhibited excellent mechanical properties, having ultimate tensile strength (UTS) and Yield strength (YS) of 346.148 Mpa and 230.8 Mpa respectively which were higher than the ideal mechanical properties necessary for vascular stent applications reported in previous literature [50], [51]. Also it had a ductility of 15.4% which is similar to the ideal 15-18% percent ductility. The improved mechanical properties of the generated Mg alloy in this study enables it to provide appropriate scaffolding and support to the injured aorta vessel wall to allow for its healing and remodeling of new blood vessels and makes it superior to ceramics and polymers in endovascular stent applications.

It was also obvious that the ANFIS model had the efficient capability of designing an Mg biodegradable alloy having the desired mechanical qualities. The addition of alloying elements had the impact of improving the strength and ductility of the Mg alloy. Moreover, the concentrations of the main alloying elements (Mg, Al, Ca, Zn, Li, Zr) did not exceed the maximum concentrations reported in previous literature, however, the concentrations of the Rare-earth elements (Y, Nd, Gd, Ho, and La) differed from other works.

For further evaluation of the mechanical aspects of the designed Mg alloy, it was compared to stainless steel which is reported as the standard stent material in several researches [15], [23], [49] and commonly studied biodegradable Mg alloys and shown in table 6. It was clear from the table that the generated Mg alloy exhibited higher tensile strength, yield strength and ductility than the other previously reported Mg alloys. The increase in the strength of the alloy can be attributed to the ability of Mg to create solid solution with many alloying elements including Ca, Mn, Al, Zn, Zr, Li and rare earth elements due to its atomic size and hexagonal close-packed system [68]. The addition of Ca, Mn, Zn and Zr provides grain refinement effect, as previously reported in the literature, due to the formation of continuous layers of
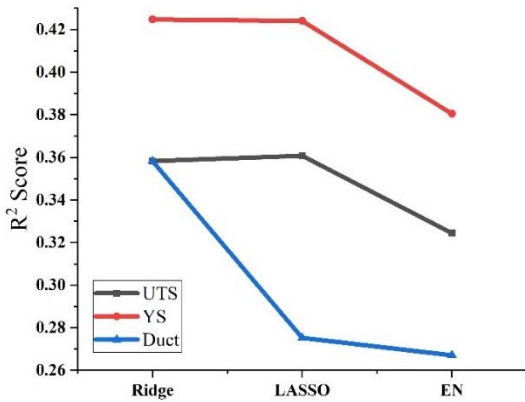
FIGURE 4. Effect of Regularization techniques on the R^2 score of the Multiple Linear Regression (MLR) models.
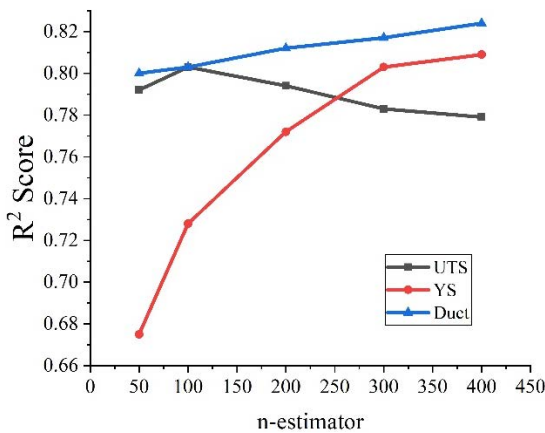

FIGURE 5. Effect of n-estimator on the R^2 score of the Gradient Boosting Regression model.

corrosion-resistant intermetallic phases around grain boundaries and hence increases the yield and tensile strength of the alloy. In addition, the small grain size particles act as barriers for the movement of dislocations during slipping and therefore can contribute to the increase in yield strength. Rare-earth elements (REEs) added to the Mg alloy have also led to the increase of strength of the generated Mg alloy as they are found to enhance the strength and corrosion resistance by both solid solution and precipitation hardening.

The YS and UTS properties of the designed Mg alloy were very close to stainless steel, which proves that it can integrate the mechanical qualities of medical stainless steel necessary for scaffolding in stent applications. Hence,

TABLE 4. The coefficients of determination R^2 score of the best fit models.

	MLR	GBR	ANFIS
UTS	0.354	0.779	0.926
YS	0.421	0.809	0.958
Ductility	0.355	0.824	0.988

TABLE 5. Compositions of the best randomly generated Mg biodegradable alloy.

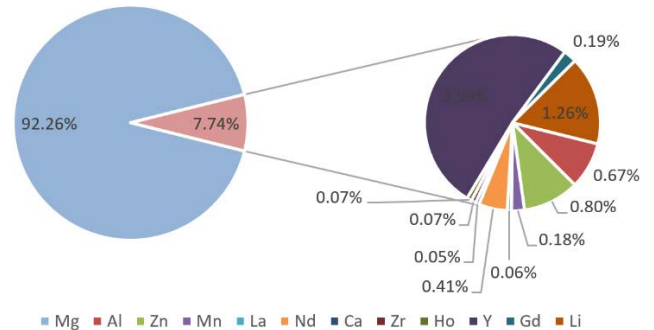|		
Composition of the Mg alloy	Mg	92.260
	Mn	0.183
	Al	0.665
	Ca	0.053
	Zn	0.801
	Li	1.260
	Zr	0.066
	Y	3.988
	Nd	0.407
	Gd	0.188
	Ho	0.070
	La	0.059
Mechanical Properties	UTS	**346.148**
	YS	**230.802**
	Duct	**15.427**

FIGURE 6. Composition of the Predicted Mg alloy.

it was concluded that the Mg biodegradable alloy designed by the ANFIS model appears to be a promising candidate that can potentially address the challenges as temporary structural biomaterials providing superior mechanical integrity essential for stent applications for Abdominal Aortic Aneurysm (AAA) repair. The evolution of Mg biodegradable stents as alternatives to non-degradable stents helps to overcome the chronic inflammatory body reactions, avoid complications, save expenses and pain to patients undergoing later re-surgeries for removal of the implanted permanent stents. Furthermore, altering the compositions of alloying elements added to Mg leads to large changes in the mechanical behavior of the alloy and the use of machine learning techniques such as the ANFIS model facilitates the design of new advanced alloys out of millions of alloys required for many medical applications reducing the time, effort and cost of large searching space.

Future enhancement of this work includes further studies that should be conducted on the implantation of biodegradable stents manufactured from the newly designed

TABLE 6. Comparison between mechanical properties of several alloys.

Metal and its Composition (Wt %)	YS (Mpa)	UTS Mpa	Ductility (%Elongation)
Stainless Steel 316L [69]	190	490	40
WE43 alloy [69]	150	250	4
AZ31 alloy [70]–[72]	185	263	15-23
AZ91 alloy [72]	160	150	2.511
WE43 [73]	170	220	2-17
Pure Mg [74]	20	86	13
New Mg alloy	230.8	346.18	15.42

Mg alloy in the abdominal aorta of some clinically approved animals for in-vivo long term evaluation. These studies should include the investigation of the healing process of the aorta vessel wall, safety, efficacy and degradation rates of the Mg alloy inside the body.

IV. CONCLUSION

In this study, Adaptive Neuro-Fuzzy Inference System (ANFIS) model was developed and compared with other classic machine learning algorithms (Multiple Linear Regression (MLR) and Gradient Boosting Regression models) for the design of an Mg biodegradable alloy necessary for Abdominal Aortic Aneurysm repair (AAAR). By evaluating the performance of the three proposed models, it was proved that the ANFIS model outperformed the other models in predicting the mechanical properties of the Mg samples with maximum R^2 scores of 0.926, 0.958, and 0.988 for UTS, YS, and Ductility respectively.

The ANFIS model efficiently predicted an Mg biodegradable alloy having improved mechanical properties of 346.148 Mpa, 230.8 Mpa, and 15.4% for UTS, YS, and Ductility which are close to the mechanical properties of stainless steel which is considered as a reference material for vascular stent applications. The results also revealed that alloying Mg with other elements such as Mn, Al, Ca, Zn, Li, Zr, and Rare-earth elements with certain compositions improved the strength and ductility of the Mg alloy which are essential requirements for the design of stents included in stent graft systems for AAAR. The biodegradable Mg stent in the stent-graft system provides a mechanical scaffold for both the graft and the aorta vessel wall and then degrades over time gradually while being metabolized in the body and replaced by the healed host aorta tissue, thus reducing any chronic inflammatory reactions caused by permanent non-degradable stents.

Hence, the ANFIS model proved to be a promising approach to accelerate the design of new alloys in the future for diverse medical applications. Furthermore, with the aid of machine learning techniques, other alloys could be designed by adding other elements to Mg with varying concentrations to further enhance its strength and ductility.

REFERENCES

[1] K. W. Johnston, R. B. Rutherford, M. D. Tilson, D. M. Shah, L. Hollier, and J. C. Stanley, "Suggested standards for reporting on arterial aneurysms," *J. Vascular Surg.*, vol. 13, no. 3, pp. 452–458, Mar. 1991.

[2] I. C. T. Santos, A. Rodrigues, L. Figueiredo, L. A. Rocha, and J. M. R. S. Tavares, "Mechanical properties of stent–graft materials," *Proc. Inst. Mech. Eng., L, J. Mater., Des. Appl.*, vol. 226, no. 4, pp. 330–341, 2012.

[3] N. T. Kouchoukos and D. Dougenis, "Surgery of the thoracic aorta," *New England J. Med.*, vol. 336, no. 26, pp. 1876–1889, 1997.

[4] K. Myers *et al.*, "Endoluminal versus open repair for abdominal aortic aneurysms," in *Proc. 2nd Virtual Congr. Cardiol.*, Argentina, Sep./Nov. 2001.

[5] M. G. A. Norwood, G. M. Lloyd, M. J. Bown, G. Fishwick, N. J. London, and R. D. Sayers, "Endovascular abdominal aortic aneurysm repair," *Postgraduate Med. J.*, vol. 83, no. 975, pp. 21–27, 2007.

[6] J. D. Blankensteijn, F. P. Lindenburg, Y. Van Der Graaf, and B. C. Eikelboom, "Influence of study design on reported mortality and morbidity rates after abdominal aortic aneurysm repair," *Brit. J. Surg.*, vol. 85, no. 12, pp. 1624–1630, Jan. 2003.

[7] R. Greenhalgh, "Comparison of endovascular aneurysm repair with open repair in patients with abdominal aortic aneurysm (EVAR trial 1), 30-day operative mortality results: Randomised controlled trial," *Lancet*, vol. 364, no. 9437, pp. 843–848, Sep. 2004.

[8] R. K. V. Sethi, A. J. Henry, N. D. Hevelone, S. R. Lipsitz, M. Belkin, and L. L. Nguyen, "Impact of hospital market competition on endovascular aneurysm repair adoption and outcomes," *J. Vascular Surg.*, vol. 58, no. 3, pp. 596–606, Sep. 2013.

[9] H. S. Rayt, A. J. Sutton, N. J. M. London, R. D. Sayers, and M. J. Bown, "A systematic review and meta-analysis of endovascular repair (EVAR) for ruptured abdominal aortic aneurysm," *Eur. J. Vascular Endovascular Surg.*, vol. 36, no. 5, pp. 536–544, Nov. 2008.

[10] S. C. Van Beek, A. P. Conijn, M. J. Koelemay, and R. Balm, "Endovascular aneurysm repair versus open repair for patients with a ruptured abdominal aortic aneurysm: A systematic review and meta-analysis of short-term survival," *Eur. J. Vascular Endovascular Surg.*, vol. 47, no. 6, p. 137, 2014.

[11] A. Dua, S. Kuy, C. J. Lee, G. R. Upchurch, and S. S. Desai, "Epidemiology of aortic aneurysm repair in the United States from 2000 to 2010," *J. Vascular Surg.*, vol. 59, no. 6, pp. 1512–1517, Jun. 2014.

[12] A. Polanczyk, M. Klinger, J. Nanobachvili, I. Huk, and C. Neumayer, "Artificial circulatory model for analysis of human and artificial vessels," *Appl. Sci.*, vol. 8, no. 7, p. 1017, Jun. 2018.

[13] A. Polanczyk, M. Podgorski, M. Polanczyk, A. Piechota-Polanczyk, C. Neumayer, and L. Stefanczyk, "A novel patient-specific human cardiovascular system phantom (HCSP) for reconstructions of pulsatile blood hemodynamic inside abdominal aortic aneurysm," *IEEE Access*, vol. 6, pp. 61896–61903, 2018, doi: 10.1109/ACCESS.2018.2876377.

[14] K. Sangeetha, A. V. J. Kumari, J. Venkatesan, A. Sukumaran, S. Aisverya, and P. N. Sudha, "Degradable metallic biomaterials for cardiovascular applications," in *Fundamental Biomaterials: Metals*. Amsterdam, The Netherlands: Elsevier, 2018, pp. 285–298.

[15] M. Moravej and D. Mantovani, "Biodegradable metals for cardiovascular stent application: Interests and new opportunities," *Int. J. Mol. Sci.*, vol. 12, no. 7, pp. 4250–4270, Jun. 2011.

[16] J. F. Dyet, W. G. Watts, D. F. Ettles, and A. A. Nicholson, "Mechanical properties of metallic stents: How do these properties influence the choice of stent for specific lesions?" *Cardiovascular Interventional Radiol.*, vol. 23, no. 1, pp. 47–54, Jan. 2000.

[17] T. Resch, M. Malina, B. Lindblad, J. Malina, J. Brunkwall, and K. Ivancev, "The impact of stent design on proximal stent-graft fixation in the abdominal aorta: An experimental study," *Eur. J. Vascular Endovascular Surg.*, vol. 20, no. 2, pp. 190–195, Aug. 2000.

[18] X.-C. Zhou, F. Yang, X.-Y. Gong, M. Zhao, Y.-F. Zheng, and Z.-L. Sun, "New nitinol endovascular stent-graft system for abdominal aortic aneurysm with finite element analysis and experimental verification," *Rare Met.*, vol. 38, no. 6, pp. 495–502, Jun. 2019.

[19] T. Tsujimura, O. Iida, M. Fujita, M. Masuda, S. Okamoto, T. Ishihara, K. Nanto, T. Kanda, S. Okuno, Y. Matsuda, M. Fujihara, Y. Yokoi, and T. Mano, "Two-year clinical outcomes post implantation of EpicTM self-expanding nitinol stents for the aortoiliac occlusive disease in patients with peripheral arterial disease," *J. Atherosclerosis Thrombosis*, vol. 25, no. 4, pp. 344–349, 2018.

[20] J. R. Laird, T. Zeller, C. Loewe, J. Chamberlin, R. Begg, P. A. Schneider, A. Nanjundappa, F. Bunch, S. Schultz, S. Harlin, A. Lansky, and M. R. Jaff, "Novel nitinol stent for lesions up to 24 cm in the superficial femoral and proximal popliteal arteries: 24-month results from the TIGRIS randomized trial," *J. Endovascular Therapy*, vol. 25, no. 1, pp. 68–78, Feb. 2018.

[21] N. Beshchasna, M. Saqib, H. Kraskiewicz, Ł. Wasyluk, O. Kuzmin, O. C. Duta, D. Ficai, Z. Ghizdavet, A. Marin, A. Ficai, Z. Sun, V. F. Pichugin, J. Opitz, and E. Andronescu, "Recent advances in manufacturing innovative stents," *Pharmaceutics*, vol. 12, no. 4, p. 349, Apr. 2020.

[22] N. Wang, K. Li, Y. Zou, and J. Wang, "Cellular response of biodegradable AZ31 magnesium alloy stent in artery," in *Proc. J. Phys., Conf.*, 2021, vol. 1732, no. 1, Art. no. 12114.

[23] L. Mao, L. Shen, J. Chen, X. Zhang, M. Kwak, Y. Wu, R. Fan, L. Zhang, J. Pei, G. Yuan, C. Song, J. Ge, and W. Ding, "A promising biodegradable magnesium alloy suitable for clinical vascular stent application," *Sci. Rep.*, vol. 7, no. 1, pp. 1–12, Jun. 2017.

[24] P. Zartner, R. Cesnjevar, H. Singer, and M. Weyand, "First successful implantation of a biodegradable metal stent into the left pulmonary artery of a preterm baby," *Catheterization Cardiovascular Interventions*, vol. 66, no. 4, pp. 590–594, 2005.

[25] X. Gu, Y. Zheng, Y. Cheng, S. Zhong, and T. Xi, "*In vitro* corrosion and biocompatibility of binary magnesium alloys," *Biomaterials*, vol. 30, no. 4, pp. 484–498, Feb. 2009.

[26] B. Heublein, "Biocorrosion of magnesium alloys: A new principle in cardiovascular implant technology?" *Heart*, vol. 89, no. 6, pp. 651–656, Jun. 2003.

[27] M. P. Staiger, A. M. Pietak, J. Huadmai, and G. Dias, "Magnesium and its alloys as orthopedic biomaterials: A review," *Biomaterials*, vol. 27, no. 9, pp. 1728–1734, Mar. 2006.

[28] W. Ding, "Opportunities and challenges for the biodegradable magnesium alloys as next-generation biomaterials," *Regenerative Biomater.*, vol. 3, no. 2, pp. 79–86, Apr. 2016.

[29] H. Hermawan, D. Dubé, and D. Mantovani, "Developments in metallic biodegradable stents," *Acta Biomater.*, vol. 6, no. 5, pp. 1693–1697, May 2010.

[30] B. Grüter, F. Strange, D. Täschler, J. Rey, M. von Gunten, D. Grandgirard, S. Leib, L. Remonda, H. R. Widmer, E. Nevzati, and others, "A biodegradable magnesium stent for aneurysm healing in a rat sidewall aneurysm model," *J. Neurol. Surg. A: Central Eur. Neurosurg.*, vol. 79, no. S1, p. O03, 2018.

[31] S. R. Peterson, "Semi-permiable biodegradable stent graft and uses thereof," U.S. Patent 12 419 508, Apr. 7, 2010.

[32] Y. Wang, M. Wei, and J. Gao, "Improve corrosion resistance of magnesium in simulated body fluid by dicalcium phosphate dihydrate coating," *Mater. Sci. Eng., C*, vol. 29, no. 4, pp. 1311–1316, May 2009.

[33] L. Petrini, W. Wu, D. Gastaldi, L. Altomare, S. Farè, F. Migliavacca, A. G. Demir, B. Previtali, and M. Vedani, "Development of biodegradable magnesium alloy stents with coating," *Frattura ed Integrità Strutturale*, vol. 8, no. 29, pp. 364–375, Jul. 2014.

[34] L. Li, J. Gao, and Y. Wang, "Evaluation of cyto-toxicity and corrosion behavior of alkali-heat-treated magnesium in simulated body fluid," *Surf. Coat. Technol.*, vol. 185, no. 1, pp. 92–98, Jul. 2004.

[35] S. Agarwal, J. Curtin, B. Duffy, and S. Jaiswal, "Biodegradable magnesium alloys for orthopaedic applications: A review on corrosion, biocompatibility and surface modifications," *Mater. Sci. Eng., C*, vol. 68, pp. 948–963, Nov. 2016.

[36] Y. C. Lee, A. K. Dahle, and D. H. StJohn, "The role of solute in grain refinement of magnesium," *Metall. Mater. Trans. A*, vol. 31, no. 11, pp. 2895–2906, Nov. 2000.

[37] Y. C. Li, M. H. Li, W. Y. Hu, P. D. Hodgson, and C. E. Wen, "Biodegradable Mg-Ca and Mg-Ca-Y alloys for regenerative medicine," *Mater. Sci. Forum*, vols. 654–656, pp. 2192–2195, Jun. 2010.

[38] Y. Ding, C. Wen, P. Hodgson, and Y. Li, "Effects of alloying elements on the corrosion behavior and biocompatibility of biodegradable magnesium alloys: A review," *J. Mater. Chem. B*, vol. 2, no. 14, pp. 1912–1933, 2014.

[39] G. L. Song and A. Atrens, "Corrosion mechanisms of magnesium alloys," *Adv. Eng. Mater.*, vol. 1, no. 1, pp. 11–33, 1999.

[40] S. Cai, T. Lei, N. Li, and F. Feng, "Effects of Zn on microstructure, mechanical properties and corrosion behavior of Mg–Zn alloys," *Mater. Sci. Eng., C*, vol. 32, no. 8, pp. 2570–2577, 2012.

[41] G. Song and D. StJohn, "The effect of zirconium grain refinement on the corrosion behaviour of magnesium-rare Earth alloy MEZ," *J. Light Met.*, vol. 2, no. 1, pp. 1–16, Feb. 2002.

[42] W. Liu, F. Cao, L. Zhong, L. Zheng, B. Jia, Z. Zhang, and J. Zhang, "Influence of rare Earth element Ce and La addition on corrosion behavior of AZ91 magnesium alloy," *Mater. Corrosion*, vol. 60, no. 10, pp. 795–803, Oct. 2009.

[43] X. Zhou, Y. Huang, Z. Wei, Q. Chen, and F. Gan, "Improvement of corrosion resistance of AZ91D magnesium alloy by holmium addition," *Corrosion Sci.*, vol. 48, no. 12, pp. 4223–4233, Dec. 2006.

[44] M. Bobby Kannan, W. Dietzel, C. Blawert, A. Atrens, and P. Lyon, "Stress corrosion cracking of rare-Earth containing magnesium alloys ZE41, QE22 and elektron 21 (EV31A) compared with AZ80," *Mater. Sci. Eng., A*, vol. 480, nos. 1–2, pp. 529–539, May 2008.

[45] P. Raccuglia, K. C. Elbert, P. D. F. Adler, C. Falk, M. B. Wenny, A. Mollo, M. Zeller, S. A. Friedler, J. Schrier, and A. J. Norquist, "Machine-learning-assisted materials discovery using failed experiments," *Nature*, vol. 533, no. 7601, pp. 73–76, May 2016.

[46] R. Ramprasad, R. Batra, G. Pilania, A. Mannodi-Kanakkithodi, and C. Kim, "Machine learning in materials informatics: Recent applications and prospects," *npj Comput. Mater.*, vol. 3, no. 1, pp. 1–13, Dec. 2017.

[47] Y. Zhang and C. Ling, "A strategy to apply machine learning to small datasets in materials science," *npj Comput. Mater.*, vol. 4, no. 1, pp. 1–8, Dec. 2018.

[48] X. Xu, L. Wang, G. Zhu, and X. Zeng, "Predicting tensile properties of AZ31 magnesium alloys by machine learning," *JOM*, vol. 72, no. 11, pp. 3935–3942, Nov. 2020.

[49] R. Balcon, R. Beyar, S. Chierchia, I. De Scheerder, P. G. Hugenholtz, F. Kiemeneij, B. Meier, J. Meyer, J. P. Monassier, and W. Wijns, "Recommendations on stent manufacture, implantation and utilization," *Eur. Heart J.*, vol. 18, no. 10, pp. 1536–1547, Oct. 1997.

[50] P. K. Bowen, E. R. Shearier, S. Zhao, R. J. Guillory, F. Zhao, J. Goldman, and J. W. Drelich, "Biodegradable metals for cardiovascular stents: From clinical concerns to recent Zn-alloys," *Adv. Healthcare Mater.*, vol. 5, no. 10, pp. 1121–1140, May 2016.

[51] R. J. Werkhoven, W. H. Sillekens, and J. B. J. M. van Lieshout, "Processing aspects of magnesium alloy stent tube," in *Magnesium Technology*, W. H. Sillekens, S. R. Agnew, N. R. Neelameggham, and S. N. Mathaudhu, Eds. Cham, Switzerland: Springer, 2011, doi: 10.1007/978-3-319-48223-1_79.

[52] J.-S. R. Jang, "ANFIS: Adaptive-network-based fuzzy inference system," *IEEE Trans. Syst., Man, Cybern.*, vol. 23, no. 3, pp. 665–685, May/Jun. 1993, doi: 10.1109/21.256541.

[53] Y. J. Wong, S. K. Arumugasamy, C. H. Chung, A. Selvarajoo, and V. Sethu, "Comparative study of artificial neural network (ANN), adaptive neuro-fuzzy inference system (ANFIS) and multiple linear regression (MLR) for modeling of Cu (II) adsorption from aqueous solution using biochar derived from rambutan *(Nephelium lappaceum)* peel," *Environ. Monit. Assessment*, vol. 192, no. 7, p. 439, 2020.

[54] N. M. Mohamad Noor and S. H. Ab Hamid, "Comparison of triangular and trapezoidal membership functions for improving decision making in crime prevention," in *DSS 2.0–Supporting Decision Making With New Technologies*. Amsterdam, Netherlands: IOS Press, 2014, pp. 69–79.

[55] O. A. M. Ali, A. Y. Ali, and B. S. Sumait, "Comparison between the effects of different types of membership functions on fuzzy logic controller performance," *Int. J.*, vol. 76, pp. 76–83, Mar. 2015.

[56] M. A. Deif, "A deep bidirectional recurrent neural network for identification of SARS-CoV-2 from viral genome sequences," *Math. Biosci. Eng.*, vol. 18, no. 6, pp. 8933–8950, 2021.

[57] T. Hastie, J. Taylor, R. Tibshirani, and G. Walther, "Forward stagewise regression and the monotone lasso," *Electron. J. Statist.*, vol. 1, pp. 1–29, Apr. 2007.

[58] B. Efron, T. Hastie, I. Johnstone, and R. Tibshirani, "Least angle regression," *Ann. Statist.*, vol. 32, no. 2, pp. 407–499, Apr. 2004, doi: 10.1214/009053604000000067.

[59] M. A. Deif, A. A. A. Solyman, and R. E. Hammam, "ARIMA model estimation based on genetic algorithm for COVID-19 mortality rates," *Int. J. Inf. Technol. Decis. Making*, vol. 20, no. 6, pp. 1775–1798, 2021.

[60] M. A. Deif, R. E. Hammam, and A. Solyman, "Gradient boosting machine based on PSO for prediction of leukemia after a breast cancer diagnosis," *Int. J. Adv. Sci. Eng. Inf. Technol.*, vol. 11, no. 2, pp. 508–515, 2021.

[61] M. A. Deif and R. E. Hammam, "Skin lesions classification based on deep learning approach," *J. Clin. Eng.*, vol. 45, no. 3, pp. 155–161, 2020.

[62] T. Hastie, R. Tibshirani, and J. Friedman, *The Elements of Statistical Learning: Data Mining, Inference, and Prediction*, 2nd ed. New York, NY, USA: Springer-Verlag, 2009.

[63] J. Friedman, T. Hastie, and R. Tibshirani, "Regularization paths for generalized linear models via coordinate descent," *J. Stat. Softw.*, vol. 33, no. 1, p. 1, 2010.

[64] M. A. Deif, A. A. A. Solyman, M. H. Alsharif, and P. Uthansakul, "Automated triage system for intensive care admissions during the COVID-19 pandemic using hybrid XGBoost-AHP approach," *Sensors*, vol. 21, no. 19, p. 6379, Sep. 2021.

[65] B. Khoshnevisan, S. Rafiee, M. Omid, H. Mousazadeh, and S. Clark, "Environmental impact assessment of tomato and cucumber cultivation in greenhouses using life cycle assessment and adaptive neuro-fuzzy inference system," *J. Cleaner Prod.*, vol. 73, pp. 183–192, Jun. 2014.

[66] H. G. Feller and Y. Kharrazi, "Cavitation erosion of metals and alloys," *Wear*, vol. 93, no. 3, pp. 249–260, Feb. 1984.

[67] K. U. Kainer, "Properties of consolidated magnesium alloy powder," *Metal Powder Rep.*, vol. 45, no. 10, pp. 684–687, Oct. 1990.

[68] H. Ibrahim, S. N. Esfahani, B. Poorganji, D. Dean, and M. Elahinia, "Resorbable bone fixation alloys, forming, and post-fabrication treatments," *Mater. Sci. Eng., C*, vol. 70, pp. 870–888, Jan. 2017.

[69] *Standard Specification for Wrought 18Chromium-14Nickel-2.5 Molybdenum Stainless Steel Bar and Wire for Surgical Implants (UNS S31673)*, West Conshohocken ASTM Int., Standard F. ASTM 138, 2003.

[70] K. Kubota, M. Mabuchi, and K. Higashi, "Review processing and mechanical properties of fine-grained magnesium alloys," *J. Mater. Sci.*, vol. 34, no. 10, pp. 2255–2262, 1999.

[71] A. Deschamps, F. Livet, and Y. Brechet, "Influence of predeformation on ageing in an Al–Zn–Mg alloy—I. Microstructure evolution and mechanical properties," *Acta Mater.*, vol. 47, no. 1, pp. 281–292, 1998.

[72] Y. Xin, T. Hu, and P. K. Chu, "*In vitro* studies of biomedical magnesium alloys in a simulated physiological environment: A review," *Acta Biomater.*, vol. 7, no. 4, pp. 1452–1459, Apr. 2011.

[73] T. Rzychoń and A. Kiełbus, "Microstructure of WE43 casting magnesium alloys," *J. Achievements Mater. Manuf. Eng.*, vol. 21, no. 1, pp. 31–34, 2007.

[74] H. Hermawan, M. Moravej, D. Dubé, M. Fiset, and D. Mantovani, "Degradation behaviour of metallic biomaterials for degradable stents," *Adv. Mater. Res.*, vols. 15–17, pp. 113–118, Feb. 2006.

MOHAMMED H. ALSHARIF received the B.Eng. degree from the Islamic University of Gaza, Palestine, in 2008, and the M.Sc. (Eng.) and Ph.D. degrees from the National University of Malaysia, Malaysia, in 2012 and 2015, respectively, all in electrical engineering (wireless communication and networking). In 2016, he joined Sejong University, South Korea, where he is currently an Assistant Professor with the Department of Electrical Engineering. His current research interests include wireless communications and networks, including wireless communications, network information theory, the Internet of Things (IoT), green communication, energy-efficient wireless transmission techniques, wireless power transfer, and wireless energy harvesting.

RANIA E. HAMMAM received the Ph.D. degree from the Chemical Engineering Department, Cairo University, in 2012. She is currently an Assistant Professor with the Bioelectronics Department, Faculty of Engineering, MTI University. Her publications were on the treatment of dyes that are present in wastewaters especially textile wastewaters by the use of cuprous oxide photocatalysts. Because of her interests and her specialization at work, she built skills in many fields of biomedical engineering, such as biomaterials, medical gas design networks inside hospitals, sterilization techniques, and clinical engineering. She is also concentrating her research in the field of biomedical and is focusing her efforts to develop herself for her postgraduate studies realizing the role of biomedical engineering in hospitals.

PEERAPONG UTHANSAKUL (Member, IEEE) received the B.Eng. and M.Eng. degrees in electrical engineering from Chulalongkorn University, Thailand, in 1996 and 1998, respectively, and the Ph.D. degree in information technology and electrical engineering from The University of Queensland, Australia, in 2007. From 1998 to 2001, he was employed as a Telecommunication Engineer in one of the leading telecommunication company of Thailand. He is currently working as an Associate Professor and the Director of the Research and Development Institute, Suranaree University of Technology, Thailand. He has got more than 300 research publications and the author/coauthor of various books related to MIMO technologies. He has won various national awards from the Government of Thailand due to his contributions and motivation in the field of science and technology. His research interests include green communications, wave propagation modeling, wireless communications, MIMO, massive MIMO, brain wave engineering, mobile networks, and quality of experience (QoE).

AHMED A. A. SOLYMAN was born in Cairo, Egypt, in 1977. He received the B.S. and M.S. degrees in communication engineering from the Military Technical College, Cairo, in 2006, and the Ph.D. degree in electrical and electronics engineering from the University of Strathclyde, U.K., in 2013.

From 2001 to 2010, he was a Research Assistant with the Military Technical Research Center. Since 2018, he has been an Assistant Professor with the Communication and Computer Engineering Department, MTI University. He is currently an Assistant Professor with the Department of Electrical and Electronics Engineering, Istanbul Gelisim University, Turkey. His Ph.D. researches in multimedia services over wireless networks using OFDM. His research interests include image processing, digital signal processing, the Internet of Things, channel estimation and equalization, wireless communication networks, and MIMO communication systems.

MOHANAD A. DEIF received the M.Sc. and Ph.D. degrees from the Biomedical Engineering Department, Helwan University, Egypt, in 2011 and 2015, respectively. He is currently an Assistant Professor with the Biomedical Engineering Department, Modern University for Technology & Information (MTI), Egypt. He worked as a Consultant in biomedical engineering with the Center for Advanced Software and Biomedical Engineering Consultations, Faculty of Engineering, Cairo University. His research interests include machine learning for biomedical applications and design of computer-aided detection software (CAD), medical space planning, and bioinformatics.

● ● ●